MEASUREMENT OF INCLUSIVE ZERO-ANGLE NEUTRON SPECTRA AT THE ISR

W. Flauger

DESY, Hamburg, Germany

F. Mönnig

Institut für Experimentelle Kernphysik, Karlsruhe, Germany

CERN, Geneva, Switzerland

Geneva - 21 January 1976

(Submitted to Nuclear Physics)

1. INTRODUCTION

For energies up to 70 GeV it has been found that the spectra of neutrons produced at zero angle in pp collisions differ significantly from the corresponding proton spectra[1]. Whereas the latter peak at the kinematic limit, the inclusive neutron spectra have a maximum at $x \approx 0.84$. This difference in behaviour casts some light on the production mechanism near the kinematic boundary, in particular on the role of pion exchange, which is expected to contribute considerably to neutron production[2].

In general, it is interesting to investigate whether Feynman scaling holds when going to ISR energies. Up to now neutron production has been measured at the ISR only at medium angles[3]. This article reports on the measurement of neutron spectra produced at zero degree for four different energies.

2. EXPERIMENTAL METHOD

Neutrons produced at 0° could leave the vacuum system of the ISR through a window of a special vacuum chamber installed in intersection 8. They were detected in a sampling total absorption counter (STAC) placed at 56 m from the interaction region. The counter used also in previous measurements of neutron spectra at the ISR is shown in Fig. 1. It consisted of a sandwich of 40 scintillator plates (40×40 cm^2) with iron plates in between; the over-all iron length was 72 cm. The light from all scintillators was guided to one 60 DVP photomultiplier. The performance of the STAC up to energies of 70 GeV has been described in detail elsewhere[4].

As indicated in Fig. 1, three trigger counters, PB0, PB1, and PB2, were inserted at a depth of 8, 12, and 52 cm of iron, respectively. The lateral dimensions of PB0 were 15×15 cm^2 and of PB1 and PB2 40×40 cm^2. The iron converter in front of PB0, which could be taken out by remote control, was restricted in area to 12×12 cm^2. In this way, the accepted angle was defined to (0 ± 1) mrad and matched the size of the window in the vacuum chamber. Also edge effects of the STAC were avoided. The taking of spectra with converter plates in and out was particularly helpful in the study of background effects, as well as to define in a proper way the efficiency of the STAC needed for the absolute normalization. Typically, the converter-out rate amounted to 50% of the converter-in rate.

The normal trigger condition consisted of a coincidence PB0PB1. With this requirement one selects showers starting in the front part of the STAC, so that they are almost completely absorbed within the counter. This could be checked by the signal from an anticounter AB placed behind the STAC.

The photomultiplier pulses of the STAC, PB0, PB1, PB2 and the anticounters AF in front of and AB behind the STAC were recorded on tape as well as the times

of flight between PB0 and several monitor counters surrounding the interaction region[5]. The ISR luminosity was monitored by means of a system of scintillators placed at both sides of the interaction region and detecting inelastic events at angles of about 50 mrad[6].

The energy calibration, detection efficiency and energy resolution of the STAC for different trigger conditions had been established in proton and electron beams[4]. During the measurements at the ISR the energy calibration was monitored with a light diode built into the light guide of the counter. Moreover, the calibration was rechecked by momentum-analysed pions coming from the interaction region[7].

In order to absorb the photons a 3 cm thick plate of lead was placed before the front anticounter AF.

The weak trigger condition PB0PB1 allowed the off-line study of background effects, especially the contamination with photons, by requiring signals from additional counters. Figure 2a shows the measured distribution for neutral particles at 52.8 GeV centre-of-mass energy. The solid points represent the original spectrum, while for the open point distribution a coincidence with the monitor counters around the interaction region was required. One notices that apart from a small low-energy background, both spectra agree in shape; the monitor system has an efficiency of about 90%. Figure 2b shows spectra taken under the same conditions but without lead in front of AF. For the lower energies the fraction of photons exceeds significantly the neutron rate.

The third spectrum in Fig. 2a was obtained with the trigger PB0PB1PB2. As the counters PB0 and PB2 were separated by about 25 radiation lengths of iron, the electromagnetic background is eliminated here to a level of less than 1%. The reduced efficiency for neutrons is taken into account.

The difference of the distributions taken without and with lead, scaled to the same monitor rate, gives the spectrum of photons produced under zero angle, see Fig. 2b. The evaluation of the cross-sections will be discussed below.

For the final analysis the distributions taken with the trigger (PB0PB1 + monitors) were used. As was shown above, by comparison with the spectra (PB0PB1) these distributions are inclusive as far as the shape is concerned, but eliminate the low-energy background present in the (PB0PB1) trigger.

The measured distributions were unfolded using experimentally determined resolution functions of the STAC. The unfolding was accomplished with standard methods[4].

The normalization was based on the Van der Meer method. The efficiency of the STAC (converter in-converter out) was corrected for back-scattering effects.

Also absorption loss in the material between interaction and detector was taken into account as well as a beam-gas contribution, which was of the order of 3-4%. No correction for dead-time due to the antis was necessary.

The K^0 background, which was subtracted, was assumed to be the average of K^+ production[8]. This background amounts to about 10% at x = 0.2 and less than 4% for x > 0.4.

3. RESULTS

Neutron spectra were taken at 30.6, 44.9, 52.8, and 62.7 GeV c.m.s. energy. The invariant cross-sections are given in Table 1 as a function of the variable $x = p/p_{max}$. The uncertainties include the statistical errors and errors from the energy calibration, the unfolding of the raw data and relative normalization errors. The over-all absolute normalization error is estimated to be ±20%, which is mostly due to the uncertainty in the efficiency of the STAC. If one extrapolates the data of Engler et al.[3] for low x to $p_T = 0$, there is agreement with the data of this experiment within the errors.

The zero-angle spectra exhibit a maximum at $x \approx 0.84$ with a relatively rapid descent to the kinematic limit. Comparing the data, for example with an unnormalized spectrum taken at 70 GeV/c laboratory momentum[1], there is no indication for an energy dependence of the invariant cross-section. In Fig. 3 two zero-angle spectra of this experiment are plotted together with data at medium angles[3] versus x.

The peak structure around x = 0.84 is not observed in the medium-angle data. This would mean a rapid decrease of the corresponding production mechanism with respect to p_T. However, the data of Ref. 3 were taken in an early stage of the ISR operation and without a special vacuum chamber; thus the background was rather high. Therefore a small bump might have been missed in the region around x = 0.8, particularly at low transverse momenta, where only relatively poor data at low energies ($\sqrt{s}$ = 22.5 and 30.6 GeV) were available[9].

Figure 4 shows the zero-angle photon spectrum for $\sqrt{s}$ = 52.8 GeV as extracted from measurements without and with the lead filter. The relatively large errors reflect the uncertainties in the energy calibration and resolution of the STAC for electrons [ratio of visible energy for electrons and protons[4]], in the detection efficiency, the absorption of the photons, and the luminosity measurements. Also previous data[10,11] at non-zero angles are shown. A constant exponential decrease with rising x is observed with an excess at small $x \lesssim 0.1$.

When analysing spectra in terms of the triple Regge model, one correlates inclusive distributions near the kinematic limit with corresponding exclusive

processes. An interesting question is therefore whether the neutron production at $p_T = 0$ can also be described by a Regge exchange mechanism, and if so, which trajectory is dominant. If the c.m.s energy squared s and the missing mass M^2 are large but M^2/s is small, the invariant cross-section can be written as[12]

$$\pi E \frac{d^3\sigma}{dp^3} \approx \frac{d^2\sigma}{dt\,d(M^2/s)} = |G(t)|^2 \left(\frac{M^2}{s}\right)^{1-2\alpha(t)} \sigma_{tot}(M^2,t) \quad . \qquad (1)$$

The Regge trajectory exchanged $\alpha(t)$ is coupled to p and n with a residue $G(t)$; $\sigma_{tot}(M^2,t)$ can be interpreted as the total Reggeon proton cross-section for a c.m.s. energy M and a Reggeon mass t, which is expected to be asymptotically constant in M^2. For $x \geq 0.88$ and $p_T = 0$ one has $|t| \leq 0.015$ $(GeV/c)^2$ for the energies of this experiment; hence for $x \geq 0.88$ the data can be treated as taken at constant $t \approx 0$. Figure 5 shows that in the region $x > 0.88$ the measured cross-sections follow indeed Eq. (1). The points very close to the kinematic limit have been omitted, since their relative error in x is rather large. Averaging over all energies one obtains an intercept $\alpha(0) = -0.11 \pm 0.15$. This small value indicates that pion exchange contributes significantly to neutron production near the kinematic boundary.

Acknowledgements

We would like to thank the members of the CERN-Roma and Pisa-Stony Brook Groups for their warm collaboration. We are indebted to J. Engler for fruitful discussions. H. Kein and K. Ratz contributed much to the success of the experiment. We thank the ISR technical support group for its help, and the ISR running staff for their efficient operation of the machine. This work was partly supported by the Bundesministerium für Forschung und Technologie, Bonn, Germany.

REFERENCES

1) V. Böhmer, J. Engler, W. Flauger, H. Keim, K. Pack, F. Mönnig, H. Schopper, A. Babaev, E. Brachman, G. Eliseev, A. Ermilov, Yu. Galaktionov, Yu. Gorodkov, Yu. Kamishkov, E. Leikin, V. Lubimov, V. Shevchenko and O. Zeldovich, Nuclear Phys. B91 (1975) 266.
J. Engler, W. Flauger, B. Gibbard, F. Mönnig, K. Pack, K. Runge and H. Schopper, Nuclear Phys. B64 (1973) 173.

2) M. Bishari, Phys. Letters 38B (1972) 510.

3) J. Engler, B. Gibbard, W. Isenbeck, F. Mönnig, J. Moritz, K. Pack, K.H. Schmidt, D. Wegener, W. Bartel, W. Flauger and H. Schopper, Nuclear Phys. B84 (1975) 109.

4) J. Engler, W. Flauger, B. Gibbard, F. Mönnig, K. Runge and H. Schopper, Nuclear Instrum. Methods 106 (1973) 189.
V. Böhmer, J. Engler, W. Flauger, H. Keim, K. Pack, F. Mönnig, H. Schopper, A. Babaev, E. Brachman, G. Eliseev, A. Ermilov, Yu. Galaktionov, Yu. Gorodkov, Yu. Kamishkov, E. Leikin, V. Lubimov, V. Shevchenko and O. Zeldovich, Nuclear Instrum. Methods 122 (1974) 313.

5) S.R. Amendolia, G. Bellettini, P.L. Braccini, C. Bradaschia, R. Castaldi, V. Cavasinni, C. Cerri, T. Del Prete, L. Foà, P. Giromini, P. Laurelli, A. Menzione, L. Ristori, G. Sanguinetti, M. Valdata, G. Finocchiaro, P. Grannis, D. Green, R. Mustard and R. Thun, Nuovo Cimento 17A (1973) 735.

6) U. Amaldi, R. Biancastelli, C. Bosio, G. Matthiae, J.V. Allaby, W. Bartel, G. Cocconi, A.N. Diddens, R.W. Dobinson and A.M. Wetherell, Phys. Letters 44B (1973) 112.

7) U. Amaldi, W. Bartel, G. Cocconi, A.N. Diddens, Z. Dimčovski, R.W. Dobinson, P. Duinker, A.M. Thorndike, A.M. Wetherell, G. Bellettini, P.L. Braccini, R. Castaldi, T. Del Prete, P. Laurelli, G. Sanguinetti, M. Valdata, A. Baroncelli, G. Matthiae, P. Grannis, H. Jöstlein, R. Kephart, D. Lloyd-Owen and R. Thun, Phys. Letters 58B (1975) 206.

8) M. Antinucci, A. Bertin, P. Capiluppi, M. D'Agostino-Bruno, A.M. Rossi, G. Vannini, G. Giacomelli and A. Bussière, Nuovo Cimento Letters 6 (1973) 121.

9) B. Robinson, K. Abe, J. Carr, J. Keyne, A. Pagnamenta, F. Sannes, I. Siotis and R. Stanek, Phys. Rev. Letters 34 (1975) 1475.

10) G. Neuhofer, F. Niebergall, J. Penzias, M. Regler, W. Schmidt-Parzefall, K.R. Schubert, P.E. Schumacher, M. Steuer and K. Winter, Phys. Letters 38B (1972) 51.

11) M. Fidecaro, G. Finocchiaro, G. Gatti, G. Giacomelli, W.C. Middelkoop and T. Yamagata, Nuovo Cimento 24 (1962) 73.

12) R.D. Peccei and A. Pignotti, Phys. Rev. Letters 26 (1971) 1076.

Table 1

Invariant cross-sections for pp → nx at 0° production angle

	$E\,d^3\sigma/dp^3$ [mb/(GeV^2/c^3)]			
x	$\sqrt{s}$ = 30.6 GeV	$\sqrt{s}$ = 44.9 GeV	$\sqrt{s}$ = 52.8 GeV	$\sqrt{s}$ = 62.7 GeV
0.15		13.7 ± 1.5	10.9 ± 1.4	9.5 ± 1.2
0.2	9.6 ± 1.6	12.8 ± 1.4	10.0 ± 1.3	8.5 ± 1.1
0.25	9.6 ± 1.4	12.2 ± 1.3	9.9 ± 1.2	8.2 ± 1.0
0.3	9.8 ± 1.3	11.9 ± 1.2	10.0 ± 1.2	8.5 ± 0.9
0.35	10.0 ± 1.3	11.9 ± 1.2	10.4 ± 1.1	8.7 ± 1.0
0.4	10.5 ± 1.3	12.3 ± 1.2	10.9 ± 1.1	9.1 ± 1.0
0.45	11.2 ± 1.3	12.7 ± 1.2	11.4 ± 1.0	9.8 ± 1.0
0.5	12.3 ± 1.2	13.6 ± 1.1	12.2 ± 1.0	11.1 ± 1.0
0.55	13.4 ± 1.2	14.8 ± 1.1	13.3 ± 1.1	12.5 ± 1.0
0.6	15.1 ± 1.2	16.4 ± 1.1	14.7 ± 1.1	14.0 ± 1.0
0.65	17.4 ± 1.3	18.2 ± 1.3	17.0 ± 1.3	15.7 ± 1.1
0.7	20.3 ± 1.3	21.0 ± 1.4	19.8 ± 1.4	17.9 ± 1.2
0.75	23.3 ± 1.6	25.5 ± 1.7	23.6 ± 1.6	21.6 ± 1.3
0.775	25.0 ± 1.7	27.8 ± 1.8	25.5 ± 1.6	23.5 ± 1.6
0.8	26.6 ± 1.8	29.1 ± 1.8	26.7 ± 1.6	25.2 ± 1.6
0.825	27.4 ± 1.8	29.2 ± 1.8	26.7 ± 1.6	26.4 ± 1.6
0.85	26.7 ± 1.9	28.0 ± 1.8	25.7 ± 1.7	26.6 ± 1.6
0.875	23.8 ± 2.5	25.3 ± 2.1	23.8 ± 1.8	25.8 ± 1.7
0.9	18.6 ± 3.0	20.9 ± 2.8	19.3 ± 2.6	23.4 ± 2.5
0.925	13.5 ± 3.0	14.9 ± 2.8	13.8 ± 2.6	16.3 ± 2.8
0.95	8.3 ± 3.0	8.3 ± 2.8	8.3 ± 2.6	9.1 ± 2.8
0.975	3.2 ± 3.0	1.8 ± 2.8	2.7 ± 2.6	1.8 ± 2.8

Figure captions

Fig. 1 : Arrangement of the STAC and counters.

Fig. 2 : Uncorrected spectra for neutral particles at $\sqrt{s}$ = 52.8 GeV a) with b) without gamma filter. The difference is due to photons.

Fig. 3 : The invariant cross-sections for neutron production as a function of the scaling variable $x = p_{\parallel}/p_{max}$. The lines are hand drawn to guide the eye.

Fig. 4 : Invariant cross-sections for photon production. The data of this experiment were taken at $\sqrt{s}$ = 52.8 GeV.

Fig. 5 : The neutron cross-sections as a function of $M^2/s \approx 1 - x$ for the momentum transfer squared $t \approx 0$.

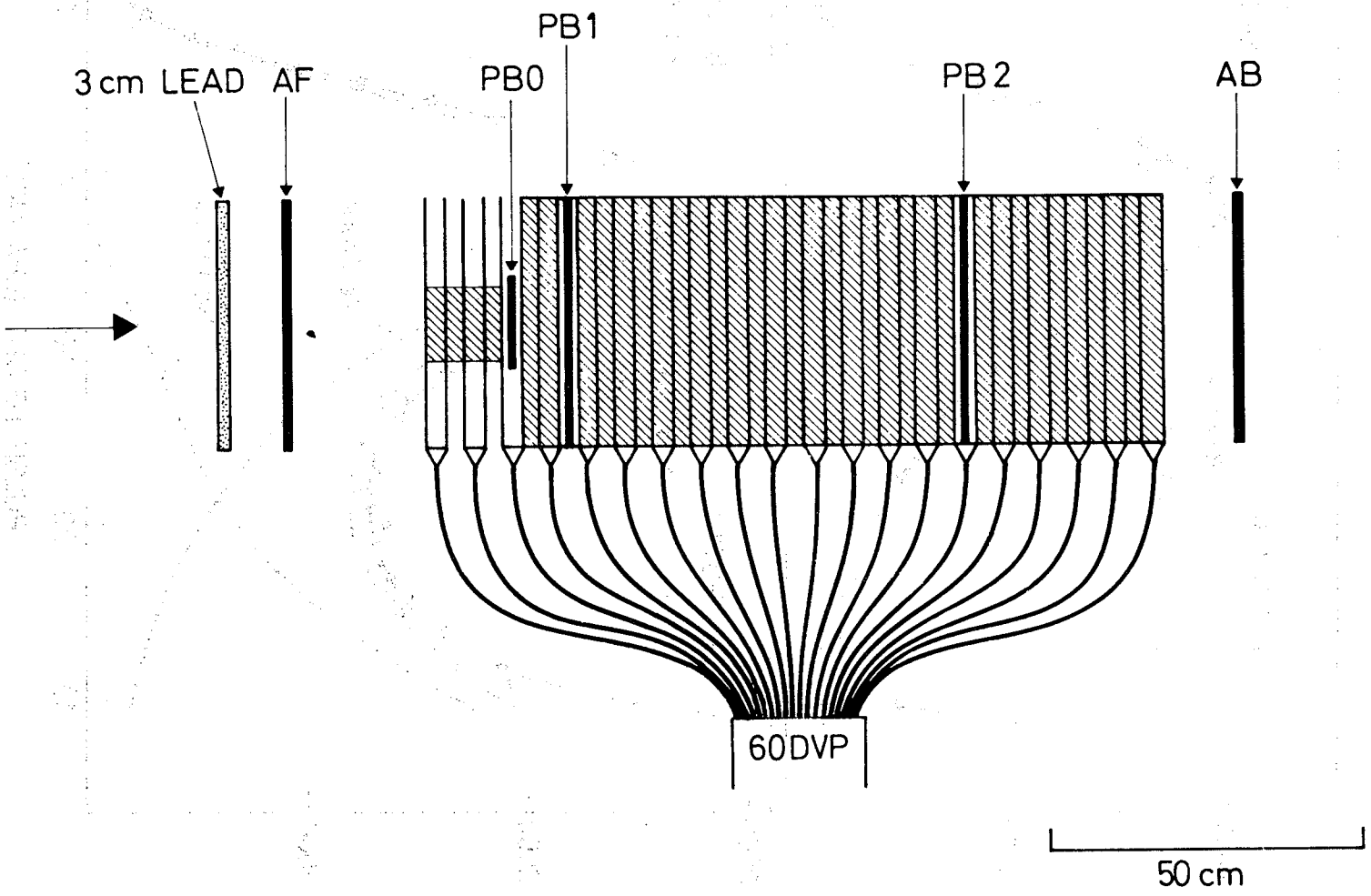

Fig. 1

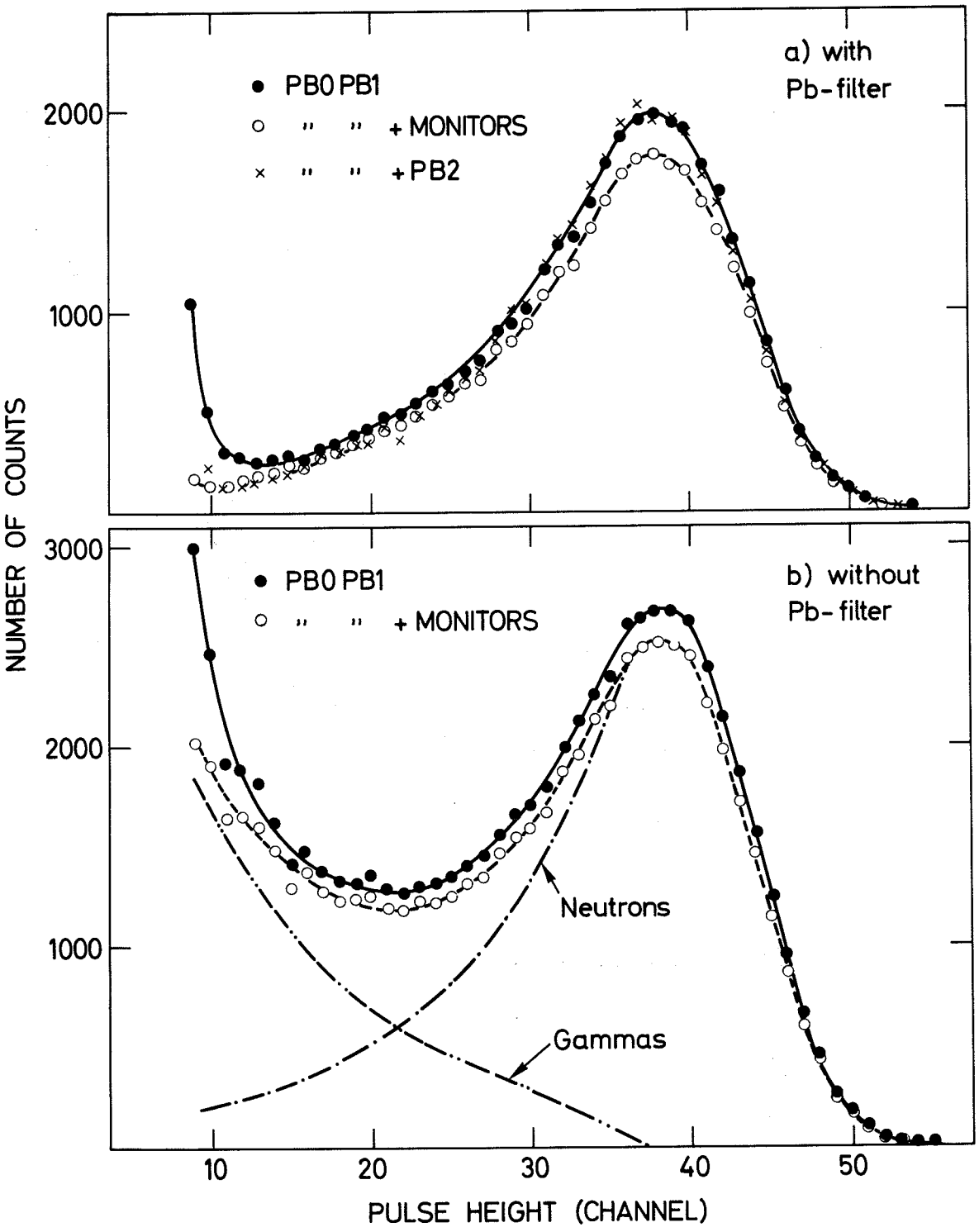
a) with
Pb-filter
PB0 PB1
" " + MONITORS
" " + PB2
2000
1000
b) without
Pb-filter
PB0 PB1
" " + MONITORS
3000
2000
1000
Neutrons
Gammas
NUMBER OF COUNTS
10
20
30
40
50
PULSE HEIGHT (CHANNEL)

Fig. 2

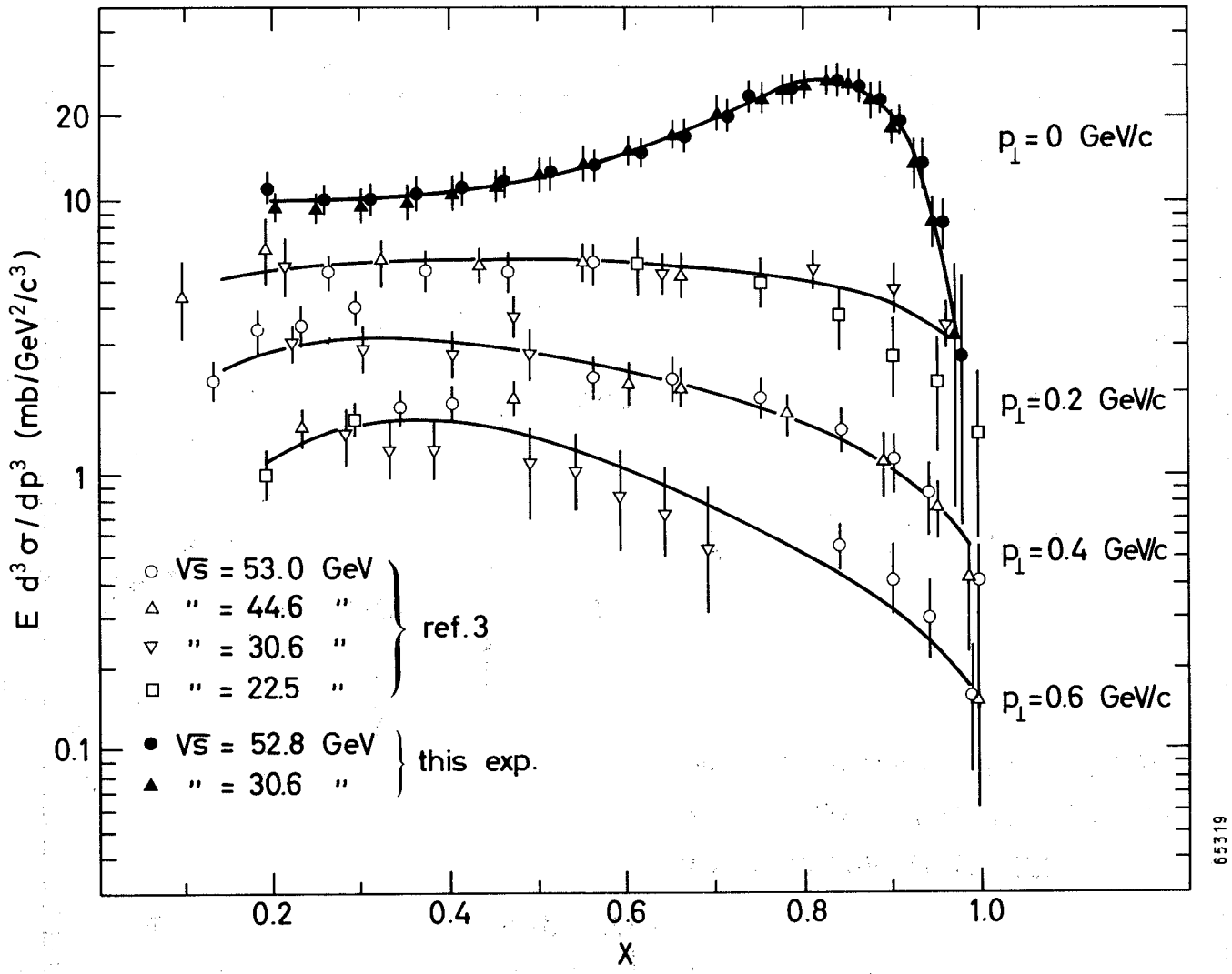
E d³σ/dp³ (mb/GeV²/c³)
20
10
1
0.1
0.2
0.4
0.6
0.8
1.0
X
p⊥ = 0 GeV/c
p⊥ = 0.2 GeV/c
p⊥ = 0.4 GeV/c
p⊥ = 0.6 GeV/c
○ √s = 53.0 GeV
△ " = 44.6 "
▽ " = 30.6 "
□ " = 22.5 "
ref. 3
● √s = 52.8 GeV
▲ " = 30.6 "
this exp.
65319

Fig. 3

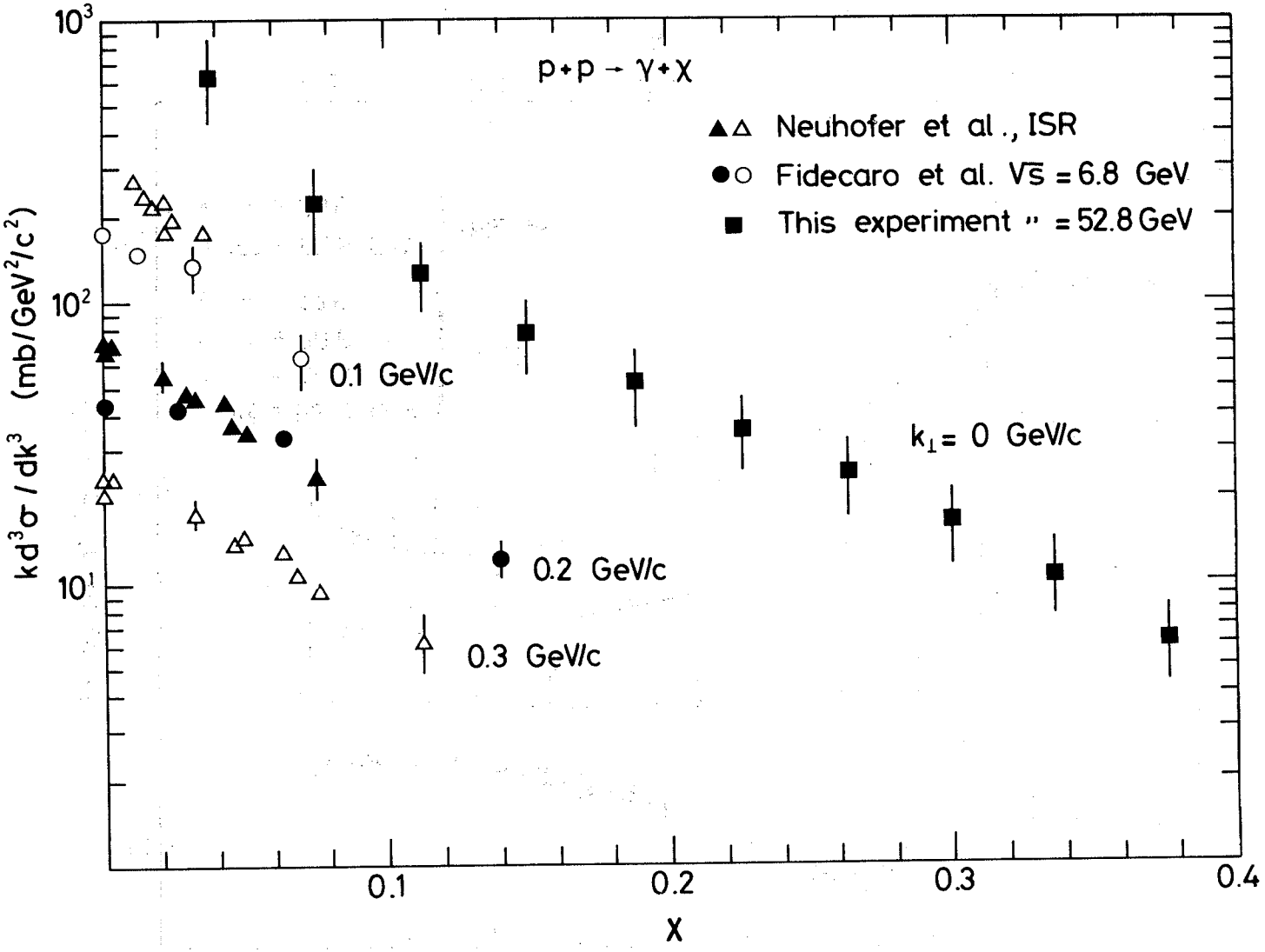
p+p → γ+X
▲△ Neuhofer et al., ISR
●○ Fidecaro et al. √s = 6.8 GeV
■ This experiment " = 52.8 GeV
0.1 GeV/c
0.2 GeV/c
0.3 GeV/c
k⊥ = 0 GeV/c
kd³σ/dk³ (mb/GeV²/c²)
10³
10²
10¹
0.1
0.2
0.3
0.4
X

Fig. 4

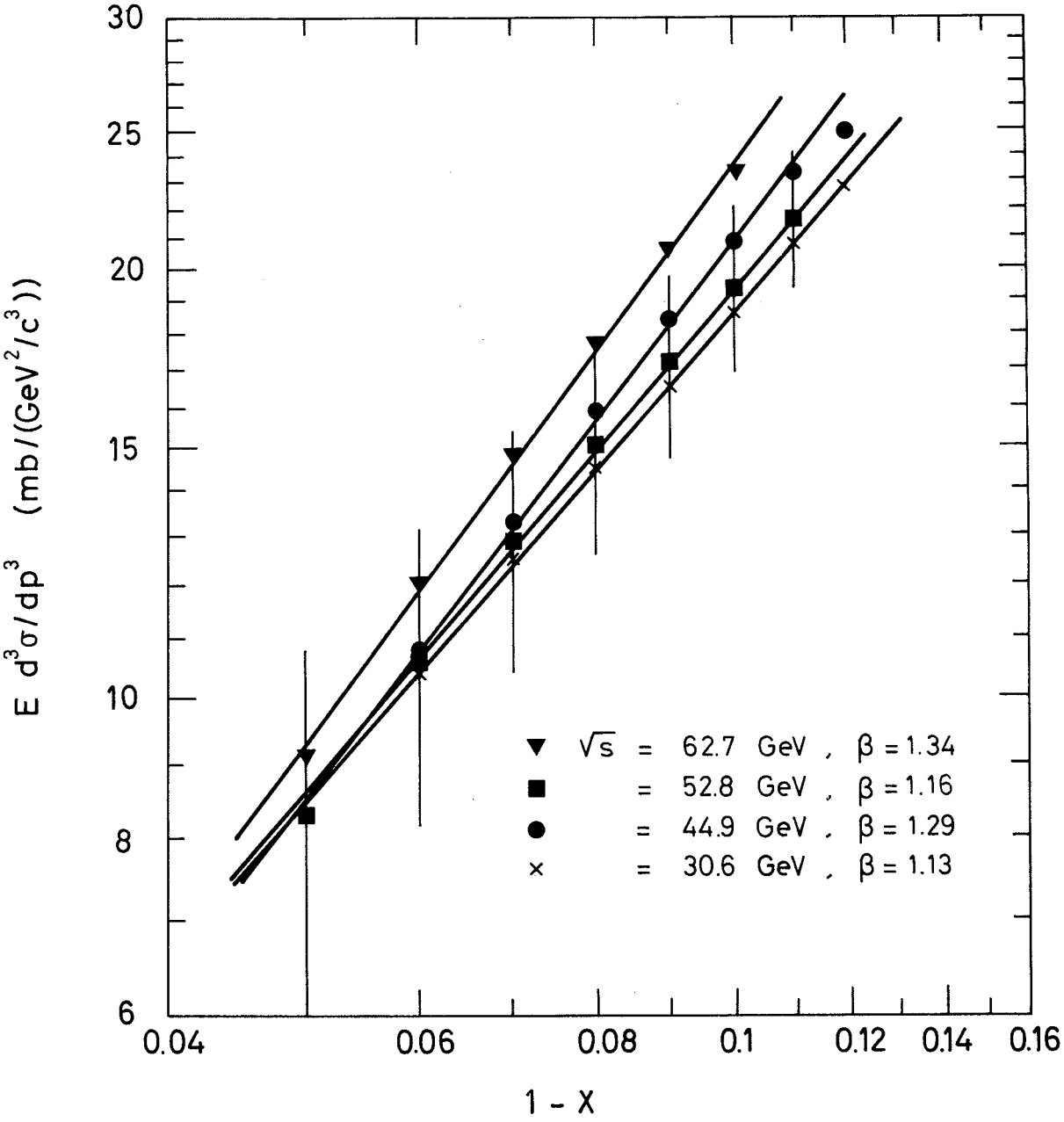
30
25
20
15
10
8
6
0.04
0.06
0.08
0.1
0.12
0.14
0.16
1 - X
E d³σ/dp³ (mb/(GeV²/c³))
√s = 62.7 GeV , β = 1.34
= 52.8 GeV , β = 1.16
= 44.9 GeV , β = 1.29
= 30.6 GeV , β = 1.13

Fig. 5

S1214